

WATER VAPOUR INTER-COMPARISON EFFORT IN THE FRAMEWORK OF THE HYDROLOGICAL CYCLE IN THE MEDITERRANEAN EXPERIMENT – SPECIAL OBSERVATION PERIOD (HYMEX-SOP1)

Donato Summa¹, Paolo Di Girolamo¹, Cyrille Flamant², Benedetto De Rosa¹, Marco Cacciani³, Dario Stelitano¹

¹ *Scuola di Ingegneria, Università degli Studi della Basilicata, Italy*, *Email: donato.summa@unibas.it

² *LATMOS/IPSL, UPMC Univ. Paris 06 Sorbonne Universités, UVSQ, CNRS, France*

³ *Dipartimento di Fisica, Università di Roma “La Sapienza”, Italy*

ABSTRACT

Accurate measurements of the vertical profiles of water vapour are of paramount importance for most key areas of atmospheric sciences. A comprehensive inter-comparison between different remote sensing and in-situ sensors has been carried out in the frame work of the first Special Observing Period of the Hydrological cycle in the Mediterranean Experiment for the purpose of obtaining accurate error estimates for these sensors. The inter-comparison involves a ground-based Raman lidar (*BASIL*), an airborne DIAL (*LEANDRE2*), a microwave radiometer, radiosondes and aircraft in-situ sensors.

1. INTRODUCTION

The ability to accurately forecast high-impact weather events, especially in the Mediterranean region, is limited by the present poor capability to properly simulate the contribution of very fine-scale processes and their non-linear interactions with the larger scale processes [1]. The improvement of weather forecasting skills requires an appropriate comprehension of the key processes influenced by the three-dimensional distribution of atmospheric water vapor and temperature. As a consequence, accurate and high-resolution global-scale measurements of the vertical profiles of water vapour mixing ratio and temperature are highly demanded [2]. Space and time resolution must be sufficiently high to allow resolving the fine structure of the atmospheric boundary layer.

Unfortunately, none of the currently available operational observational techniques for measuring water vapour and temperature

tropospheric profiles (radiosounding, microwave radiometry, Global Navigation Satellite System) is characterized by the necessary measurement capability and performances (Wulfmeyer et al., 2015 [3]). Only lidar systems exploiting the differential absorption (DIAL) and Raman techniques have the potential to overcome these limitations, thus providing high-precision low-bias water vapour and temperature profile measurements with sufficiently high vertical and temporal resolution.

For the purpose of characterizing the performances of lidar systems and demonstrating their capabilities in terms of measurement precision and accuracy, comprehensive inter-comparison efforts involving lidars and other sensors measuring the same atmospheric parameters are required. This paper illustrates results from a specific inter-comparison effort dedicated to water vapour sensors carried out in the frame work of the first Special Observing Period of the Hydrological cycle in the Mediterranean Experiment (HyMeX-SOP1) [4].

2. METHODOLOGY

Different water vapour sensors were operated in the frame of HyMeX-SOP1. The University of *BASIL*icata ground-based Raman Lidar system (*BASIL*) was deployed in the Cévennes-Vivarais site (Candillargues, Southern France, Lat: 43°37' N, Long: 4° 4' E, Elev: 1 m) and operated between 5 September and 5 November 2012, collecting more than 600 hours of measurements, distributed over 51 measurement days and 19 intensive observation periods (IOPs). *BASIL* is capable to perform high-resolution and accurate

where i is an index denoting the intercomparison sample, $q_1(z)$ and $q_2(z)$ are the water vapour mixing ratio values from the two sensors at height z , z_1 and z_2 are the lower and upper boundary of the considered height interval, respectively, and N_z is the total number of data points for each sensor in the interval $[z_1, z_2]$. Profiles of mean bias and RMS deviations are computed considering the total number of possible intercomparisons for each sensors' pair.

Table 1: Intercomparison BASIL and LEANDRE2: the first and second column identify date and time of the intercomparison, respectively; the third column identifies the flight number and IOP; the fourth column identifies the minimum distance between BASIL and the ATR42 footprint (expressed in km), the fifth and sixth column identify the relative bias and RMS deviation

Date (2012)	Time (UTC)	Flight / IOP	Min. Dis. (km)	Mean bias (%)	Mean RMS (%)
11 Sept.	11:31	34 / IOP 1	0.13	-20	32
23 Sept.	14:19	39 / IOP 5-6	28.02	-21,80	45,20
23 Sept.	17:06	39 / IOP 5-6	61.05	-22,90	33,60
26 Sept.	06:16	40 / IOP 7a	26.21	-6,4	21,60
26 Sept.	09:24	40 / IOP 7a	34.27	6,45	20,10
28 Sept.	15:07	41 / IOP 8	28.29	-6,67	30,20
28 Sept.	20:15	41 / IOP 8	63.42	-11,60	29,70
02 Oct.	21:00	42 / IOP 9	6.17	-1,06	11,30
02 Oct.	21:10	42 / IOP 9	7.13	-2,54	13,20
02 Oct.	21:20	42 / IOP 9	7.92	2	11,40
02 Oct.	21:25	42 / IOP 9	8.38	-3,82	12,60
02 Oct.	21:30	42 / IOP 9	7.83	0,15	9,20
02 Oct.	21:35	42 / IOP 9	7.66	-2,19	9,4
11 Oct.	06:45	43 / IOP 12a	145.1	-4,28	37,10
11 Oct.	09:43	43 / IOP 12a	38.78	-1,66	21,20
12 Oct.	01:18	44 / IOP 12b	28.45	-6,46	11,90
12 Oct.	06:57	45 / IOP 12b	38.17	-1,78	8,10
14 Oct.	08:28	46 / IOP 13	28.00	4,30	24,60
14 Oct.	15:27	47 / IOP 13	22.25	16,10	30,40
15 Oct.	05:24	48 / IOP 13	27.59	14,50	11,60
18 Oct.	15:43	51 / IOP 14	26.39	16,1	26,10
18 Oct.	19:02	51 / IOP 14	38.29	7,41	19,1
20 Oct.	10:03	52 / IOP 15a	37.58	3,93	36

(expressed in %) between the two sensors, respectively.

To apply equation (1) and (2) a common height array has to be considered for each sensors' pair. Equations (1) and (2) allow computing the relative, or percentage, bias and RMS deviation. These quantities allow quantifying the mutual performances of the two compared sensors, i.e. the performance of one sensor with respect to the other. This approach attributes equal weight to the data reliability of each sensor and it is particularly appropriate when none of the two compared sensors can *a priori* be assumed to be more accurate than the other one [12].

Comparisons between BASIL and LEANDRE2 were possible on a variety of case studies. This effort benefitted from the dedicated ATR42 flights in the frame of the EUFAR Project "WaLiTemp". In addition to these dedicated flights, LEANDRE 2 data from additional HyMeX flights were used for intercomparison purposes (see complete list in Table 1). Due to eye-safety issues, LEANDRE 2 has been acquiring nadir profiles only once the ATR was flying higher than 2 km above surface.

Specifically, Table 1 lists the date and time of the intercomparison, the number of the flight and corresponding IOP number, the minimum distance between BASIL and the ATR42 footprint, as well as the relative bias and RMS deviation (expressed in %) between the two sensors, respectively. The table reveals that single bias values do not exceeding 20 %, with an average value of -2.65%, while single RMS values are not exceed 45% with an average value of 21%.

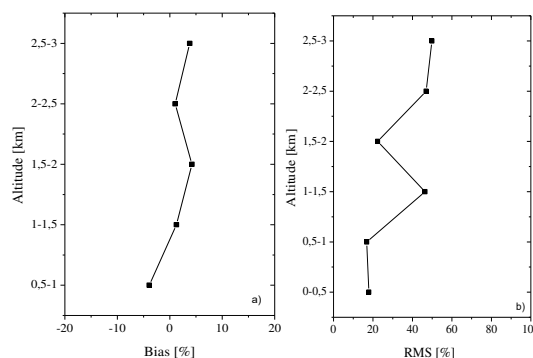


Figure 2: Relative bias (panel a) and RMS deviation (panel b) of BASIL vs. the water vapour in-situ sensor (expressed in %)

Intercomparison between BASIL and other sensors were also carried out. Figure 2 illustrates the mean bias (left panel) and RMS deviation (right panel) of BASIL vs. the water vapour in-situ sensor on-board the ATR42 aircraft. Mean bias and RMS deviation between these two sensors are -1.17% and 33.41 %, respectively, while mean bias and RMS deviation of BASIL vs. radiosondes are -1.8% and 21%, respectively. Additional results considering with all possible sensors' pairs will be illustrated and presented.

ACKNOWLEDGEMENTS

This work is a contribution to the HyMeX programme supported by MISTRALS and ANR IODA-MED Grant ANR-11-BS56-0005. This research effort was supported by the European Commission under the European Facility for Airborne Research programme of the seventh Framework Programme (Project WaLiTemp).

References

- [1] Kalthoff, N., M. Kohler, C. Barthlott, B. Adler, S.D. Mobbs, U. Corsmeier, K. Träumner, T. Foken, R. Eigenmann, L. Krauss, S. Khodayar and P. Di Girolamo, 2011. The dependence of convection-related parameters on surface and boundary-layer conditions over complex terrain, *Q. J. Roy. Meteor. Soc.* **137**, 70-80, doi: 10.1002/qj.686.
- [2] Wulfmeyer V., H. Bauer, P. Di Girolamo, C. Serio, 2005: Comparison of active and passive water vapour remote sensing from space: An analysis based on the simulated performance of IASI and space borne differential absorption Lidar, *Remote Sens. Environ.* **95**, 211-230, doi: 10.1016/j.rse.2004.12.019.
- [3] Wulfmeyer, V., R. M. Hardesty, D. D. Turner, A. Behrendt, M. P. Cadeddu, P. Di Girolamo, P. Schlüssel, J. Van Baelen, and F. Zus, 2015: A review of the remote sensing of lower tropospheric thermodynamic profiles and its indispensable role for the understanding and the simulation of water and energy cycles, *Rev. Geophys.* **53**, 819–895, doi:10.1002/2014RG000476.
- [4] Di Girolamo, P., C. Flamant, M. Cacciani, E. Richard, V. Ducrocq, D. Summa, D. Stelitano, N. Fourrié and F. Saïd, 2016: Observation of low-level wind reversals in the Gulf of Lion area and their impact on the water vapour variability, *Q. J. Roy. Meteor. Soc.* **142** (Suppl 1), 153–172, doi: 10.1002/qj.2767.
- [5] Di Girolamo, P., D. Summa, R. Ferretti, 2009: Multiparameter Raman Lidar Measurements for the Characterization of a Dry Stratospheric Intrusion Event, *J. Atmos. Ocean. Tech.* **26**, 1742-1762, doi: 10.1175/2009JTECHA1253.1.
- [6] Summa D., Di Girolamo P., Stelitano D. and Cacciani M., 2013: Characterization of the Planetary boundary layer height and structure by Raman lidar: Comparison of different approach, *Atmos. Meas. Tech.* **6**, 3515-3525, doi: 10.5194/amt-6-3515-2013.
- [7] P. Di Girolamo, D. Summa, B. De Rosa, M. Cacciani, A. Scoccione, A. Behrendt, V. Wulfmeyer, 2017: Characterization of Boundary Layer Turbulent Processes by Raman Lidar: Demonstration of the Measurement Capabilities of the Raman Lidar System BASIL, *Atmos. Chem. Phys.* **17**, 745-767, doi:10.5194/acp-17-745-2017.
- [8] P. Di Girolamo, P., A. Behrendt, and V. Wulfmeyer (2006). Spaceborne profiling of atmospheric temperature and particle extinction with pure rotational Raman Lidar and of relative humidity in combination with differential absorption Lidar: performance simulations, *Appl. Opt.* **45**, 2474-2494, ISSN: 0003-6935, doi: 10.1364/AO.45.002474.
- [9] Di Girolamo P., D. Summa, R.-F Lin, T. Maestri, R. Rizzi, G. Masiello, 2009: UV Raman Lidar measurements of relative humidity for the characterization of cirrus cloud microphysical properties, *Atmos. Chem. Phys.* **9**, 8799-8811, doi: 10.5194/acp-9-8799-2009.
- [10] Bruneau D, Quaglia P, Flamant C, Meissonnier M, Pelon J., 2001: Airborne lidar LEANDRE II for water-vapor profiling in the troposphere. I: System description, *Appl. Opt.* **40**, 3450–3461.
- [11] Bruneau D, Quaglia P, Flamant C, Pelon J., 2001b: Airborne lidar LEANDRE II for water-vapor profiling in the troposphere. II: First results. *Appl. Opt.* **40**, 3462–3475.
- [12] Bhawar, R., P. Di Girolamo, D. Summa, C. Flamant, D. Althausen, A. Behrendt, C. Kiemle, P. Bossler, M. Cacciani, C. Champollion, T. Di Iorio, R. Engelmann, C. Herold, Müller, D., S. Pal, M. Wirth, V. Wulfmeyer, 2011: The Water Vapour Intercomparison Effort in the Framework of the Convective and Orographically-Induced Precipitation Study: Airborne-to-Ground-based and airborne-to-airborne Lidar Systems, *Q. J. Roy. Meteor. Soc.* **137**, 325–348, doi:10.1002/qj.697.